

Short Communication

# High-temperature Aging Behavior of Commercial Li-Ion Batteries

Xiaoyi Xie, Li Wang<sup>\*</sup>, Xuning Feng, Dongsheng Ren, Xiangming He<sup>\*</sup>

Institute of Nuclear & New Energy Technology, Tsinghua University, Beijing 100084, China

<sup>\*</sup>E-mail: [wang-l@tsinghua.edu.cn](mailto:wang-l@tsinghua.edu.cn) ; [hexm@tsinghua.edu.cn](mailto:hexm@tsinghua.edu.cn)

Received: 3 January 2020 / Accepted: 26 February 2020 / Published: 10 April 2020

---

Herein, we report high-temperature aging behavior of commercial Li-ion batteries (LIBs) after heating at 100 °C in which environment. After thermal aging, the results reveal a capacity drop of 61.1% during initial 2 charge/discharge cycles, however, the capacity started to recover after the 2<sup>nd</sup> cycle and became stable after 24<sup>th</sup> cycle. In 16 charge/discharge cycles, we have observed a capacity recovery rate of 94.5%. The recovery rate linearly increased during initial four charge/discharge cycles, followed by an exponential decrease. The present report demonstrates that thermal aging can be accelerated by increasing the aging temperature, which is an efficient and fast route for performance evaluation of LIBs.

---

**Keywords:** high-temperature aging; Li-ion batteries; capacity retention; capacity recovery rate

## 1. INTRODUCTION

Commercial lithium-ion batteries (LIBs), first developed in 1990, have been become essential for our daily life for a wide range of applications, including laptops, cellular phones and household appliances. Moreover, LIBs are promising candidates for large-scale applications, such as electric vehicles and grid energy storage. However, the decline in battery capacity over time determines the cell performance, cyclic life and calendar life [1-4]. Therefore, the actual storage and working conditions should be considered for performance evaluation. For instance, the operating temperature significantly influences the battery aging and failure. The elevated temperature leads to electrolyte decomposition and increases the impedance of interface [3, 5-8], leading to rapid capacity decay. The aging behavior of LIBs has been studied in the temperature range of 30 to 60 °C [7-17], however, the aging experiments at >70 °C have not been attempted yet.

Herein, we tried to establish the upper-temperature limit for aging experiments, where higher cell stability and lesser time are employed as fundamental criteria. Consequently, a new method is presented to estimate the cell performance in shorter times.

## 2. EXPERIMENTAL SECTION

### 2.1. Cell fabrication and characterization

Commercial 16 Ah NCM ( $\text{LiNi}_{1/3}\text{Mn}_{1/3}\text{Co}_{1/3}\text{O}_2$ ) pouch cells were characterized by using a LAND Battery Testing System (CT2001B, Wuhan LANHE Co. Ltd., China).

The batteries were activated by carrying out the charge/discharge process at 0.2 C for 3 cycles. The cells were rested for 1 h after the activation to minimize the polarization. Then, the cells are charged at 1 C to SOC100% using CC (constant current)-CV (constant voltage) method. SOC 100% was defined by the cut-off voltage of 4.2 V and current limit of 3%I ( $I = 16 \text{ A}$ ). Again, the cells were rested for 1 h to ensure the stability of SOC.

The 100% charged cells were soaked in a thermostat (Zhongxing Weiye Co., Ltd) at 100 °C for 1.5 h, followed by natural cooling for 5 h. Then, the charge/discharge cycling was carried out by using LAND Battery Testing System. The data collection scheme is illustrated in Fig. 1.

### 2.2. Data Sampling

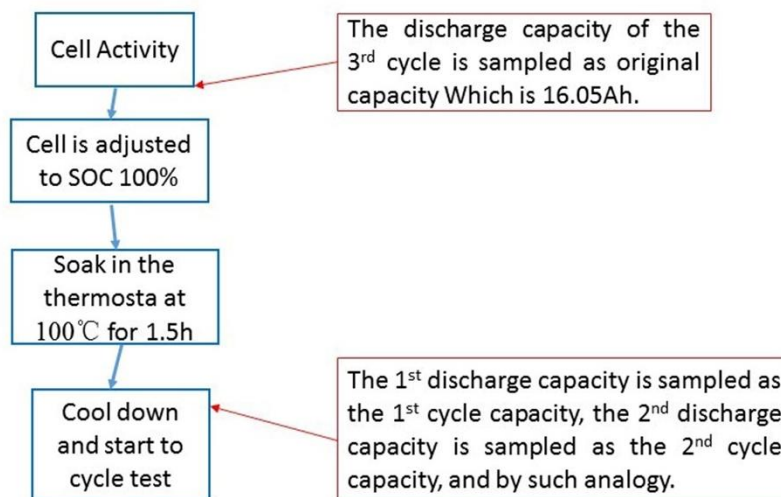


**Figure 1.** The data collection scheme utilized in current experiments.

## 3. RESULTS AND DISCUSSION

### 3.1. Capacity decay

The capacity, capacity retention and capacity loss after aging at 100 °C for 1.5 h are shown in Fig. 2. The capacity retention and capacity loss were calculated by using the given relationships:

$$\text{Capacity retention} = C_1/C_0 * 100\% \quad (1)$$

$$\text{Capacity recovery} = C_n/C_0 * 100\% \quad (2)$$

$$\text{Capacity loss} = (C_0 - C_n) / C_0 * 100\% \quad (3)$$

where  $C_1$  refers to the 1<sup>st</sup> discharge capacity after heating at 100 °C;  $C_n$  represents the n<sup>th</sup> cycle capacity after heating at 100 °C; and  $C_0$  corresponds to the original capacity. After aging at 100 °C, the commercial LIB delivered the 1<sup>st</sup> discharge capacity of 11.5 Ah, which corresponds to a capacity retention of 71.86% and capacity loss of 28.14%. Moreover, the 2<sup>nd</sup> discharge capacity was found to be 9.8 Ah, which corresponds to the capacity retention of 61.1%. Obviously, the high-temperature aging influenced the LIBs and (de)insertion of Li-ions between cathode and anode was hindered during initial two charge/discharge cycles. However, the capacity started to recover from the 3<sup>rd</sup> charge/discharge cycle and the LIB delivered a capacity of 15.1Ah after 24<sup>th</sup> charge/discharge cycle, which corresponds to a capacity retention of 94.5%. Moreover, the capacity remained stable during subsequent charge/discharge cycles.

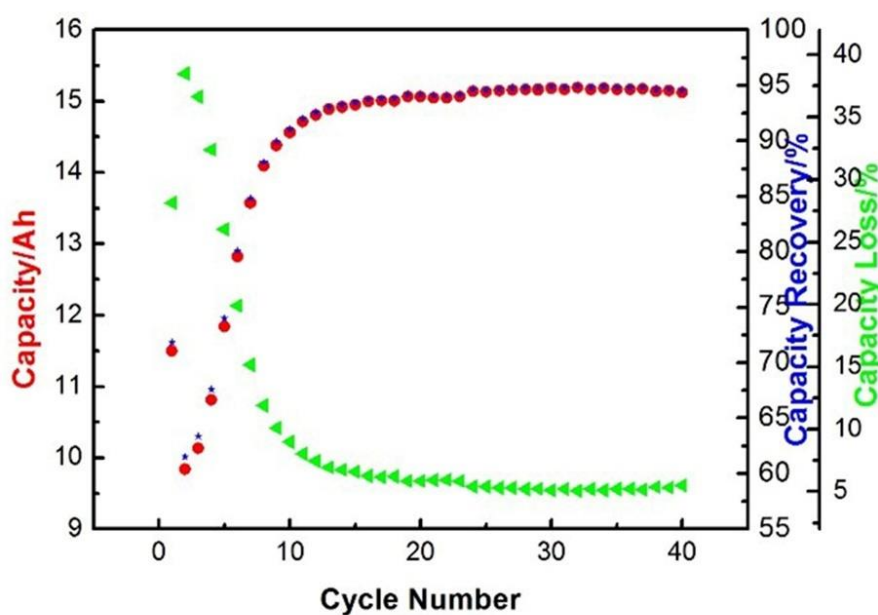


**Figure 2.** Capacity, capacity retention and capacity loss after storage in 100 °C for 1 h.

Previously, the aging behavior of LIBs is reported in the temperature range of 30 to 60 °C [7-17] and rare studies have been carried out at >70 °C. However, high-temperature stability is usually investigated at >100 °C [6, 18-20]. It has been reported that the reactions begin around 60 °C in the charged state, leading to battery failure due to temperature-induced irreversible decomposition of solid electrolyte interface (SEI) and LiPF<sub>6</sub> electrolyte [21-24]. These results indicate the occurrence of two types of changes, reversible and irreversible, at 100 °C. Owing to the reversible nature of some changes, 95% of the cell capacity has been recovered during initial 24 charge/discharge cycles. The proposed research strategy is an efficient way of accelerating the aging process, which facilitates the performance evaluation of LIBs.

3.2 Capacity recovery rate

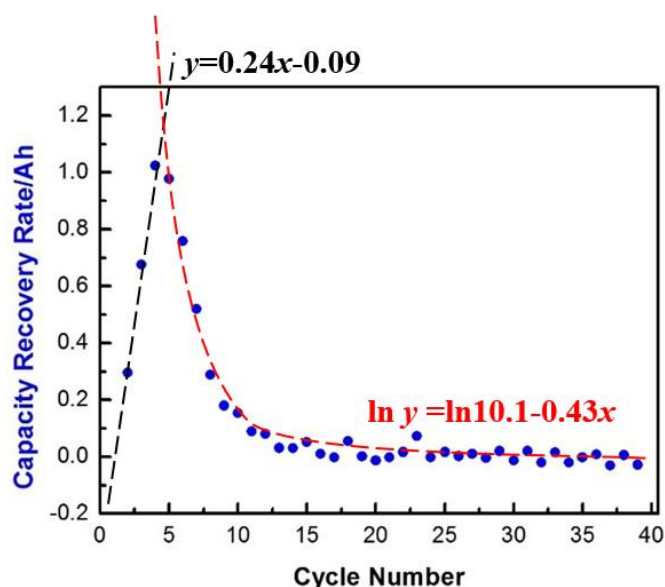


Figure 3. Capacity recovery rate after storage at 100 °C.

The capacity recovery rate (CRR) can be defined as:

$$CRR = (C_{n+1} - C_n) / (Cycle_{n+1} - Cycle_n) \quad (4)$$

where  $C_n$  is the capacity of battery at the cycle  $n$ .

Fig. 3 shows that the capacity recovery started from the 2<sup>nd</sup> charge/discharge cycle. The recovery rate linearly increased during initial 4 charge/discharge cycles, which can be given as:

$$y = 0.24x - 0.09$$

where the change in capacity was found to be 0.38 Ah, which is 2.38% of the original capacity.  $y$  is the capacity of battery at the cycle  $x$ . After 4<sup>th</sup> charge/discharge cycle, the capacity recovery rate started to decrease, which can be given as:

$$\ln y = \ln 10.1 - 0.43x$$

After 9<sup>th</sup> charge/discharge cycle, the capacity recovery rate has been decreased to 0.13 Ah per cycle and became stable 24<sup>th</sup> charge/discharge cycle. Hence, the thermally-aged cells, at 100 °C, recovered the initial capacity after 24 charge/discharge cycles, confirming the occurrence of reversible changes during high-temperature storage.

4. CONCLUSIONS

In summary, we have studied the thermal aging of commercial Li-ion batteries (LIBs) at 100 °C. After thermal aging, the cell capacity was dropped to 61.1% during initial 2 charge/discharge cycles, indicating the hindered (de)insertion of Li-ions in active electrode materials due to thermal aging. However, the capacity started to recover after 2<sup>nd</sup> charge/discharge cycle and became stable after 24<sup>th</sup>

charge/discharge cycle, corresponding to a capacity recover rate of 94.5%. The capacity recovery rate linearly increased during initial 4 charge/discharge cycles, followed by an exponential decrease. The excellent recovery rate indicates the occurrence of both reversible and irreversible reactions during high-temperature aging, however, further work is required to identify the reaction mechanisms during aging process. The current work demonstrates an excellent strategy to accelerate the aging process, increase the upper-temperature limit and reduce the experimental time for performance evaluation of LIBs.

#### ACKNOWLEDGMENTS

This work was funded by the Ministry of Science and Technology of China (No. 2019YFE010200, 2019YFA0705703 and 2018YFB0104400), the National Natural Science Foundation of China (No. U1564205 and 51706117), the China Postdoctoral Science Foundation (No. 2017M610086), the Beijing Municipal Program (No. YETP0157) and the Tsinghua University Initiative Scientific Research Program (No. 2019Z02UTY06). Moreover, authors would like to thank Joint Work Plan for Research Projects under the Clean Vehicles Consortium at U.S. and China – Clean Energy Research Center (CERC-CVC2.0, 2016-2020) and Tsinghua University-Zhangjiagang Joint Institute for Hydrogen Energy and Lithium Ion Battery Technology (JIHLT).

#### References

1. X. Feng, C. Weng, X. He, X. Han, L. Lu, D. Ren, M. Ouyang, *Ieee Transactions on Vehicular Technology*, 68 (2019) 8583-8592.
2. J. Cannarella, C.B. Arnold, *J. Power Sources*, 269 (2014) 7-14.
3. J. Vetter, P. Novák, M.R. Wagner, C. Veit, K.C. Möller, J.O. Besenhard, M. Winter, M. Wohlfahrt-Mehrens, C. Vogler, A. Hammouche, *Journal of Power Sources*, 147 (2005) 269-281.
4. H.H. (USABC), V.B. (LBNL), J.C. (INEEL), I.B. (ANL), G.H. (INEEL), E.T. (SNL), in: U.S.D.o. Energy (Ed.), 2005.
5. J. Shim, *Journal of Power Sources*, 112 (2002) 222-230.
6. S. Komaba, L. Croguennec, F. Tournadre, P. Willmann, C. Delmas, *The Journal of Physical Chemistry C*, 117 (2013) 3264-3271.
7. K. Jalkanen, J. Karppinen, L. Skogström, T. Laurila, M. Nisula, K. Vuorilehto, *Applied Energy*, 154 (2015) 160-172.
8. H. Song, Z. Cao, X. Chen, H. Lu, M. Jia, Z. Zhang, Y. Lai, J. Li, Y. Liu, *Journal of Solid State Electrochemistry*, 17 (2012) 599-605.
9. Q. Wang, J. Sun, X. Yao, C. Chen, *Thermochimica Acta*, 437 (2005) 12-16.
10. M.-S. Wu, P.-C.J. Chiang, J.-C. Lin, *Journal of The Electrochemical Society*, 152 (2005) A1041.
11. I.Bloom, B.W.Cole, J.J.Sohn, S.A.Jones, E.G.Polzin, *Journal of Power Sources*, 101 (2001) 238-247.
12. N. Omar, Y. Firouz, H. Gualous, J. Salminen, T. Kallio, J.M. Timmermans, T. Coosemans, P. Van den Bossche, J. Van Mierlo, (2015) 263-279.
13. M.A. Danzer, V. Liebau, F. Maglia, (2015) 359-387.
14. M. Kassem, J. Bernard, R. Revel, S. Péliissier, F. Duclaud, C. Delacourt, *Journal of Power Sources*, 208 (2012) 296-305.
15. M. Ecker, N. Nieto, S. Käbitz, J. Schmalstieg, H. Blanke, A. Warnecke, D.U. Sauer, *Journal of Power Sources*, 248 (2014) 839-851.
16. S. Käbitz, J.B. Gerschler, M. Ecker, Y. Yurdagel, B. Emmermacher, D. André, T. Mitsch, D.U. Sauer, *Journal of Power Sources*, 239 (2013) 572-583.

17. S.S. Choi, H.S. Lim, *Journal of Power Sources*, 111 (2002) 130–136.
18. M. Takahashi, H. Ohtsuka, K. Akuto, Y. Sakurai, *Journal of The Electrochemical Society*, 152 (2005) A899.
19. J. Lamb, C.J. Orendorff, K. Amine, G. Krumdick, Z. Zhang, L. Zhang, A.S. Gozdz, *Journal of Power Sources*, 247 (2014) 1011-1017.
20. T.-Y. Lu, C.-C. Chiang, S.-H. Wu, K.-C. Chen, S.-J. Lin, C.-Y. Wen, C.-M. Shu, *Journal of Thermal Analysis and Calorimetry*, 114 (2013) 1083-1088.
21. J.-I. Yamakia, I. Yamazakib, M. Egashiraa, S. Okadaa, *Journal of Power Sources* 102 (2001) 288-293.
22. C. Arbizzani, G. Gabrielli, M. Mastragostino, *Journal of Power Sources*, 196 (2011) 4801-4805.
23. W. Lu, Z. Chen, H. Joachin, J. Prakash, J. Liu, K. Amine, *Journal of Power Sources*, 163 (2007) 1074-1079.
24. H. Maleki, *Journal of The Electrochemical Society*, 146 (1999) 3224.

© 2020 The Authors. Published by ESG ([www.electrochemsci.org](http://www.electrochemsci.org)). This article is an open access article distributed under the terms and conditions of the Creative Commons Attribution license (<http://creativecommons.org/licenses/by/4.0/>).